American Mineralogist, Volume 87, pages 1607–1615, 2002

Berthierine/chamosite, corrensite, and discrete chlorite from evolved verdine and evaporite-associated facies in the Jurassic Sundance Formation, Wyoming

P.C. RYAN[1,*] AND S. HILLIER[2]

[1]Geology Department, Middlebury College, Middlebury, Vermont 05753, U.S.A.
[2]Macaulay Land Use Research Institute, Craigiebuckler, Aberdeen, AB15 8QH, U.K.

ABSTRACT

Late Jurassic sandstones of the shallow-marine Sundance Formation contain authigenic chlorite minerals that occur as rosette-like pore fillings of interstratified berthierine/chamosite (B-C) and honeycomb-like pore linings of corrensite and discrete chlorite. B-C is nearly ubiquitous in Sundance sandstones, but is absent near the top of the formation, whereas corrensite and discrete chlorite were detected only in uppermost Sundance sandstones, within 4 m of the contact with the overlying non-marine Morrison Formation. Glauconite grains are common and occur as laminae along bedding planes and cross-beds, indicating reworking and deposition as clasts in tidally influenced regimes.

The mineralogical, chemical, and morphological properties of the B-C and corrensite indicate that they are authigenic and formed during burial diagenesis from precursor minerals, odinite in the case of B-C, and saponite in the case of corrensite and discrete chlorite. Odinite has been recognized in numerous shallow-marine sands of the Holocene verdine facies, and the shallow-marine conditions associated with Sundance deposition would have been ideal for odinite formation. Saponite commonly forms in aeolian and evaporitic environments, implying that the saponite precursor to corrensite and discrete chlorite formed in uppermost Sundance sands that were exposed to an influx of oxidizing groundwater following regression of the Sundance sea.

X-ray diffraction (XRD) indicates that the proportion of 7 Å B layers in B-C ranges from 5 to 28%, and chemical analysis by scanning electron microscope-energy dispersive X-ray spectrometry (SEM-EDS) indicates positive correlation between %B and Fe/(Fe + Mg). The polytype of the B-C is *Ibb*, and the corrensite and discrete chlorite are disordered *IIb*. These are the expected polytypes and %B for sandstones exposed to burial diagenetic conditions of 3000–4000 m and temperatures 90–120 °C.

INTRODUCTION

Modern shallow-marine sediments in tropical environments are known to contain two authigenic green clay facies, the verdine and glaucony facies (Odin 1985, 1988, 1990). The verdine facies is distinguished by the presence of the authigenic clay mineral odinite (Bailey 1988a), a disordered Fe^{+3}-rich mineral with a 7 Å *d*(001), and other less-common minerals including 10 and 14 Å trioctahedral forms (Bailey 1988a; Odin 1990; Amouric et al. 1995; Wiewiora et al. 1999). The verdine facies has been documented most commonly in Holocene and late Pleistocene (<20 Ka) sediments on shallow continental shelves (commonly 10–60 m water depth), prodeltas, lagoons, and estuaries between 23 °S and 16 °N latitude (Odin and Sen Gupta 1988; Odin 1990; Rao et al. 1995; Kronen and Glenn 2000). Additional characteristics of the environment of formation include a water temperature of approximately 25 °C, oxidizing water immediately above the sediment, normal salinity, a pH range of 7.5–8.5, proximity to rivers rich in Fe, high sedimentation rate, sandy sediment, and reducing microenvironments (e.g., dissolution cavities, fecal pellets) (Bailey 1988a). Older odinite specimens (e.g., 10^4 y) tend to have greater proportions of interstratified 14 Å layers than do younger specimens (e.g., 10^3 y), and based on this observation, Bailey (1988a) suggested that the unstable odinite transforms to a more chlorite-like mineral upon shallow burial. Little is known about the fate of odinite in sediments older than Miocene age (Odin 1990; Wiewiora et al. 1999). Most likely, verdine facies sediments are the precursor to sedimentary ironstones (Odin 1990) and sandstones with pore-lining diagenetic chlorites (e.g., Ehrenberg 1993; Hillier 1994). Odinite is believed to transform to chlorites with randomly interstratified 7 Å berthierine-like layers (Hornibrook and Longstaffe 1996; Ryan and Reynolds 1996). This conclusion is further supported by recent work of Aagaard et al. (2000), who documented: (1) the transformation of poorly crystalline 7 Å Fe-rich clay to grain-coating chlorite in laboratory syntheses, and (2) the formation of grain-coating chlorite at 90 °C at the expense of Fe-rich poorly crystalline precursors in North Sea sandstones. Above 90 °C, these minerals exhibit compositional and structural changes that include transformation of 7 Å berthierine-like layers to 14 Å chamosite-like layers via an R0 mixed-layer series as well as transformation from the *Ibb* polytype to either the *IIb* polytype (e.g. Karpova 1969, Hillier 1994, Spotl et al. 1994) or the *Iaa* polytype (Ryan and Reynolds 1996).

Minerals of the glaucony facies (primarily 10 Å glauconite and Fe-rich smectites) form under different conditions than verdine, particularly with respect to water depth, latitude, and

* E-mail: pryan@middlebury.edu

proximity of the depositional environment to rivers (Porrenga 1967; Odin 1985; Odin and Sen Gupta 1988; Odin 1990). In contrast to the shallow depth of formation of odinite, glauconite commonly forms at the sediment-seawater interface at the shelf-slope break, where sedimentation rates are low, water depths are >100 m, and temperatures are 10–15 °C (Odin 1988). Glauconite is also less restricted geographically, forming at latitudes as high as 60°. A good example of the relationship between the verdine and glaucony facies is given by Porrenga (1967), who examined green granules in Holocene shallow marine sediments from the Niger and Orinoco deltas. Odinite (originally termed chamosite by Porrenga) and glauconitic smectite were identified in sediments sampled from water depths of 10–50 and 125–250 m, respectively. The odinite was described as Fe-rich and poorly ordered with a dominant 7 Å reflection; the glauconitic smectite contained 70% expandable layers and its XRD characteristics resembled Fe-rich smectite. Subsequent research by Odin and coworkers (e.g., Odin and Giresse 1972; Odin 1985, 1988, 1990; Odin et al. 1988) documented similar relationships between odinite and glauconitic minerals in the Congo River delta, on the continental shelf between the Orinoco and Amazons Rivers, in New Caledonia, and in other shallow-marine environments close to the mouths of rivers (Odin 1990). More recent studies have documented similar relationships in marine sediments from off-shore India and Australia (e.g., Rao et al. 1995; Kronen and Glenn 2000).

In this paper, we seek to assess relationships between interstratified berthierine-chamosite (B-C) rosettes, which are nearly ubiquitous in Sundance Formation sandstones, and pore-lining corrensite and discrete chlorite, which are present only in sandstones from the upper 4 m of the Sundance Formation. We also address the presence of glauconite, which is also nearly ubiquitous in the Upper Sundance Formation. XRD, SEM-EDS, and stratigraphic analysis are used to assess the possibility that the Sundance Formation represents an evolved analog of the verdine facies, and to further assess the idea that the corrensite originated as saponite that formed in the presence of oxidizing, evaporitic groundwater produced by marine regression. In addition to analyzing the origins of these clays, we also examine the chemical composition, mixed-layering, and polytypism of the B-C, corrensite and discrete chlorite, parameters that are often used to assess diagenetic and metamorphic grade (e.g., Cathelineau 1985; de Caritat et al. 1993; Jiang et al. 1994; Hillier 1994; Ryan and Reynolds 1996; Shata and Hesse 1998).

Materials and methods

Sandstone beds of the upper Sundance Formation (Late Jurassic) were sampled from outcrops in the Bighorn Basin of north-central Wyoming and the eastern Wind River basin. The Bighorn Basin is located between 43.5–44.5 °N and 107–108.5 °W, and the Wind River Basin is located between 42.5–43.5 °N and 107–108.5 °W. The Sundance Formation is divided informally into lower and upper members, with each representing a major transgressional/regressional marine sequence (Picard 1993). The focus of this study is the tabular sandstone beds of the Upper Sundance Formation, which were deposited in tidal flats, tidal inlets, and sandy shoals (Uhlir et al. 1988). Sundance sediments were deposited at a paleolatitude of ~35 °N in a warm and arid to semi-arid climate (Picard 1993). The Upper Sundance Formation in the study area varies from 15 to 30 m thick (Uhlir 1987; Uhlir et al. 1988). In one case (Lander Dome, eastern Wind River Basin), a well-exposed stratigraphic section was sampled from the lower part of the Upper Sundance Formation up through the contact with the overlying fluvial and lacustrine Morrison Formation. Stratigraphic relationships of these formations are shown on Figure 1. Estimated burial depth of the Sundance Formation prior to the Laramide Orogeny is 3000–4000 m and is based on: (1) current 3000 m burial depth of Sundance Formation obtained from numerous oil wells in the central Bighorn Basin and elsewhere (Peterson 1957), and (2) stratigraphic thicknesses of pre-Laramide sedimentary rocks atop the Sundance Formation in the study area (Steidtmann 1993). Under a normal geothermal gradient of 25 °C/km and a surface temperature of 20 °C, this implies maximum diagenetic temperatures of approximately 90–120 °C.

Specimens were crushed gently and without grinding, and then sonified in a water bath to enhance disaggregation. The 1–2 μm and <1 μm fractions were obtained by gravity settling in Atterberg cylinders. In order to assess mixed-layering of glauconite and chlorite minerals, oriented mounts of these two size

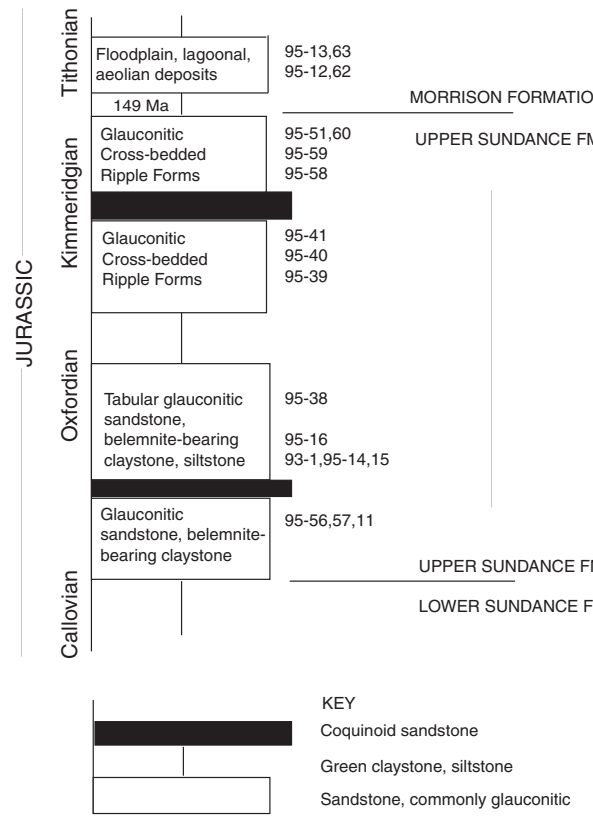

Figure 1. Stratigraphic relationship of upper Sundance Formation and lower Morrison Formation. Thickness of the upper Sundance Formation in the study area ranges from 15 to 30 m. The 149 Ma date at the base of the Morrison Formation is based on fission track analyses of Chen (1989) and paleomagnetic data of Swierc and Johnson (1996). Approximate stratigraphic position of samples is indicated.

fractions were prepared for XRD analysis by the filter peel method of Drever (1973). Polytypism was assessed by analysis of random powder mounts produced by spray drying (Hillier 1999). XRD analyses were performed on a Siemens/Bruker D-5000 diffractometer using Co$K\alpha$ radiation and a diffracted beam monochromater. The beam was collimated with 1° divergence and antiscatter slits and a 0.2° receiving slit.

Recognition and quantification of 7–14 Å chlorite (B-C) mixed-layering was carried out according to the method of Reynolds et al. (1992) and by comparison to NEWMOD-calculated patterns (Reynolds 1985). The presence of corrensite was assessed by comparing experimental XRD patterns to published patterns of Reynolds (1988), Hillier (1993), and Roberson et al. (1999), and to calculated patterns generated by NEWMOD (Reynolds 1985). The presence of glauconite was assessed by comparison to data in Moore and Reynolds (1997), and mixed-layering was assessed by comparison of experimental XRD patterns to NEWMOD-generated patterns. Polytype analyses were performed on spray-dried powders of the 1–2 μm and <1 μm fractions, and were interpreted by comparing XRD results to published data (e.g., Bailey 1988b; Hillier 1994; McCarty and Reynolds 1995; Ryan and Reynolds 1996) and patterns calculated using WILDFIRE (Reynolds 1993).

Scanning electron microscopy (SEM) was used to examine textural and spatial relationships of authigenic and detrital minerals. Samples were prepared by gold-coating rock chips mounted on aluminum stubs. Mineral compositions (major elements) were assessed by SEM-EDS (energy dispersive X-ray spectrometry) analysis of rock chips on a Philips XL30 CP SEM using a standard-based ZAF correction program. Average chemical composition for each mineral specimen represents the average of 10 separate point analyses, and results were reproducible to the extent that 1σ values are ±6% of mean values for each mineral specimen. Rather than present results as wt% oxides, we present data in terms of elemental ratios, specifically Fe/(Fe + Mg), Al:Fe, and Al:Mg. Our rationale for this approach is that the compositional analyses were performed on rock chips rather than polished sections and, although elemental ratios are expected to be precise (Curtis et al. 1985), oxide totals are well below expected chlorite values of 85–88 wt%.

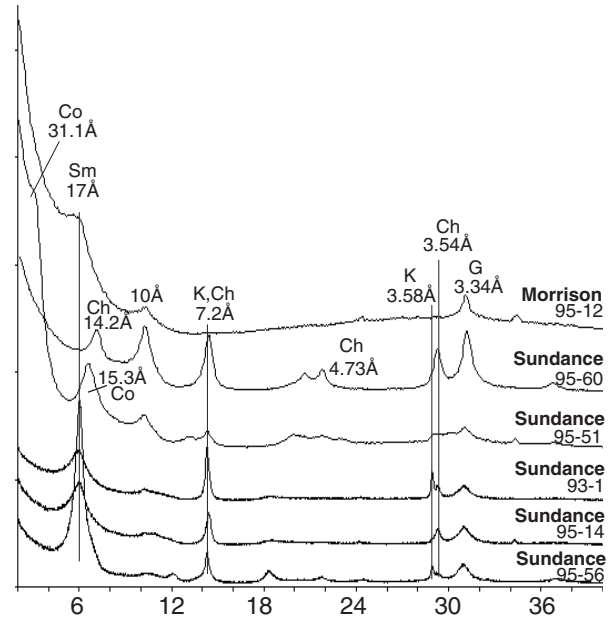

FIGURE 2. Representative XRD patterns of the <1 μm fraction, upper Sundance and basal Morrison Formations. Patterns are arranged from the lower part of the upper Sundance Formation (95-56, at bottom) up through the upper Sundance Formation and to the basal Morrison Formation (95-12, at top). Note occurrence of: (**a**) B-C in the 3 bottom patterns (evidenced by broad odd-order chlorite peaks—see Fig. 3A), (**b**) corrensite (31.1, 15.3 Å peaks) in 95-51, (**c**) discrete chlorite in 95-60 (indicated by sharp odd-order chlorite peaks at 14.1 and 4.72 Å), and (**d**) predominance of 17 Å smectite in the basal Morrison Formation (95-12). The 3.58 Å peak is from kaolinite and the 3.54 Å peak is from chlorite (discrete chlorite or B-C). The 17 Å peak is the smectite 001, the 10 Å peak is the glauconite 001 except in 95-12, where it is illite, and the 7.2 Å peak is the combined chlorite 002 and kaolinite 001. Data are from oriented, ethylene glycol-solvated specimens. Calcite = cc, chlorite = Ch, corrensite = Co, glauconite = G, kaolinite = K, quartz = Q, smectite = Sm. Co$K\alpha$ radiation.

RESULTS

XRD analyses indicate a clay mineral suite that consists of chlorite minerals, glauconite, smectite, kaolinite, and illite (Fig. 2, Table 1). Minor amounts of calcite, detrital mica, and quartz are also present in the <1 and 1–2 μm fractions.

Berthierine-Chamosite (B-C)

Ten out of fifteen Upper Sundance sandstones analyzed in this study contain a chlorite mineral that consists of R0 interstratification of 7 and 14 Å Fe-rich chlorite layers. Odd-order chlorite peaks are broadened relative to even-order peaks (Fig. 3A), a characteristic that is distinctive of mixed-layer 7–14 Å sedimentary diagenetic chlorites (Reynolds et al. 1992; Hillier 1994; Ryan and Reynolds 1996). There is no consensus on the proper nomenclature of this mineral, for it has been referred to as serpentine-chlorite (Reynolds et al. 1992; Ryan and Reynolds 1996; Banfield and Bailey 1996), Fe-rich chlorite with interstratified 7 Å layers (Hillier 1994), and berthierine-chlorite (Ahn and Peacor 1985). The term serpentine-chlorite describes the diagenetic 7–14 Å chlorites at the group level but does not indicate the unique chemical and structural properties of these minerals. In sedimentary and diagenetic environments these minerals are so consistently Fe-rich and trioctahedral (e.g., Hillier 1994) that the more precise term berthierine-chamosite (B-C) is preferable. If Mg-rich, 7–14 Å clays occur in sandstones, they have yet to be described.

The proportion of 7 Å B layers in B-C varies from 5 ± 1% to 28 ± 3%, and all B-C specimens are the *Ibb* polytype (Fig. 3B). Crystals occur as pore-filling rosettes (Fig. 3C), and all B-C specimens are Fe-rich (Table 2). Those with the highest percentage of B layers (22–35%) have the highest Fe/(Fe + Mg) ratios (0.80–0.87), whereas specimens with <8% B layers have lower Fe/(Fe + Mg) ratios (0.70–0.75) (Fig. 4, Table 2). Al:Fe ratios for B-C range from 0.69–1.86 and show no sys-

tematic variation with %B layers. These compositions are similar to B-C minerals from other sandstones (Jahren and Aagaard 1989; Reynolds et al. 1992; Hillier 1994; Ryan and Reynolds 1996).

Coexisting with rosettes of B-C in one specimen (95-39) are subhedral flakes or platelets of a berthierine-like clay (Fig. 3D) with anomalously high Fe/(Fe + Mg) ratios of 0.90 to 0.97 and low Al:Fe ratios of 0.11 to 0.40, but they contain no K, Ca, or Na. These crystals are morphologically unique in that they exist as isolated small (<5 μm) platelets rather than as aggregated crystals in rosettes or isopachous pore-linings. XRD analyses of specimen 93-39 indicate the presence of B-C and glauconite, but we have no XRD data specific to these relatively rare crystals.

Corrensite and discrete chlorite

Samples of sandstone collected from the uppermost 4 m of the Sundance Formation contain pore lining corrensite and discrete chlorite but no B-C (Fig. 5A). Discrete chlorite is recognized in XRD patterns by 00*l* peaks (14.2, 7.1, 4.73, 3.54, 2.84 Å) that do not exhibit odd-order broadening and are unaffected by ethylene glycol and heating to 300 °C. Corrensite is recognized in XRD patterns by the presence of a 31.1 Å 001 peak and a 15.3 Å 002 peak produced by regular R1 interstratification of 14 Å chlorite layers and 17 Å smectite layers (ethylene glycol-solvated). When heated to 300 °C, these specimens are characterized by diagnostic peaks at 12.2 (002) and 8.1 Å (003) (Roberson et al. 1999). The polytype of the corrensite is disor-

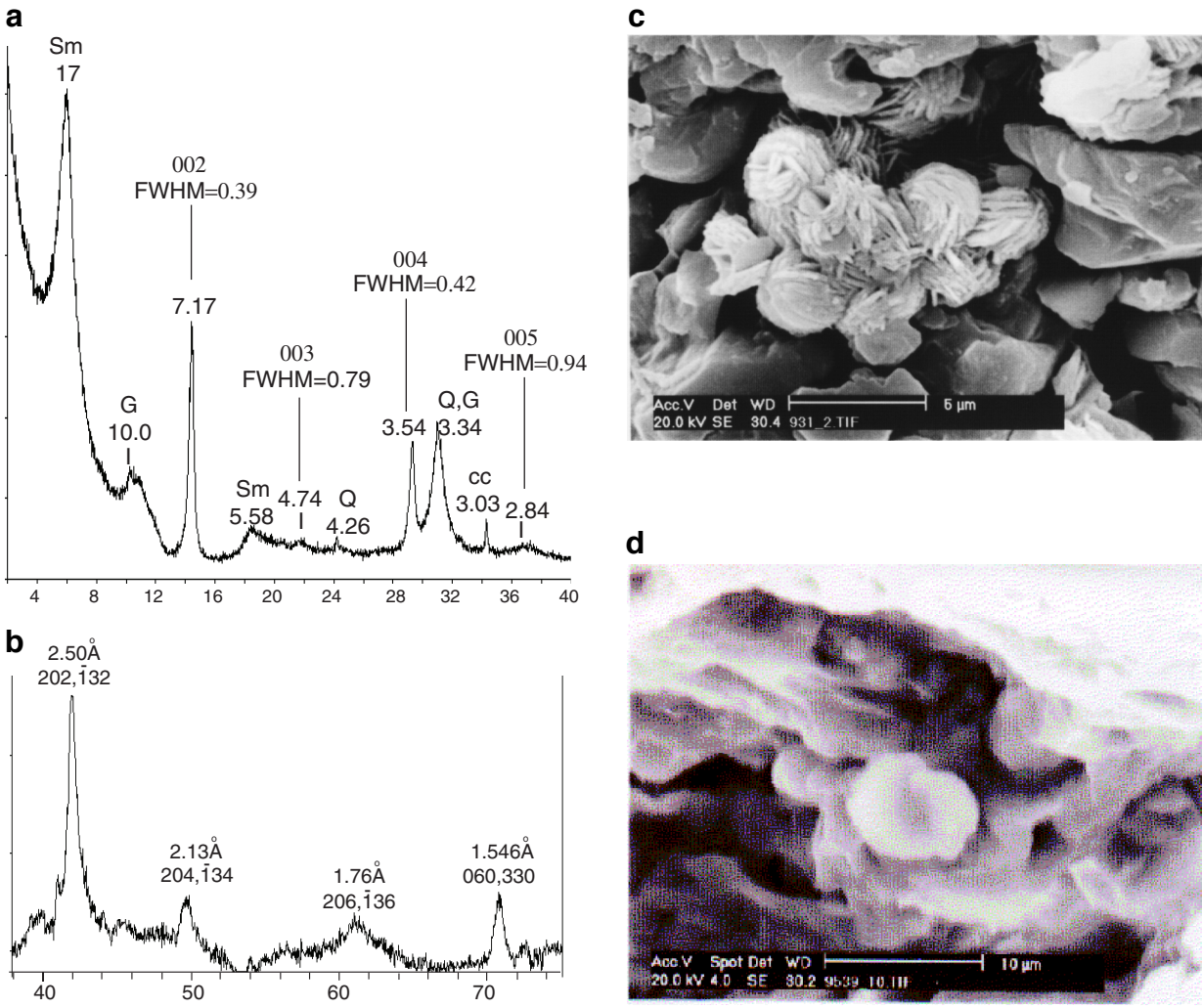

FIGURE 3. (**a**) Peak broadening of odd-order chlorite peaks produced by interstratification of 7 and 14 Å layers—shown here are peak breadths at half-height (full width at half maximum—FWHM) for the 002, 003, 004, and 005 peaks. This B-C contains 15 ± 2% 7 Å layers. The sample is 95-15, a friable, olive-green sandstone. Oriented, ethylene glycol-solvated preparation, <1 μm, Co*K*α radiation. (**b**) *Ibb* polytype typical of Sundance Formation 7–14 Å chlorites, sample 95-15. This pattern was produced using differential XRD and subtracting quartz and glauconite from the XRD pattern of the spray-dried <1 μm fraction. Co*K*α radiation. (**c**) SEM image of pore-filling, rosette-like B-C (7–14 Å chlorite), center of image, sample 93-1. (**d**) SEM image of clay crystal (center of image, adjacent to quartz clast) with very high Fe/(Fe + Mg) ratio of 0.95.

TABLE 1. Sample numbers, sample locations, and clay mineral assemblages (<1 micrometer fraction)

Sample ID	Formation	Location	Clay minerals
95-13	Morrison	Lander Dome	S
95-12	Morrison	Arminto	S, K
95-63	Morrison	Lander Dome	S, I
95-62	Morrison	Lander Dome	S
95-60	Sundance	Lander Dome	G, Ch
95-51	Sundance	Arminto	Co, Ch
95-59	Sundance	Lander Dome	G, Ch, Co
95-58	Sundance	Lander Dome	Sm, G, K, tr Ch
95-41	Sundance	Thermopolis	G, S, Be-Ch
95-40	Sundance	Lander Dome	G, S, Be-Ch
95-39	Sundance	Lander Dome	G, S, Be-Ch
95-38	Sundance	Lander Dome	G, S, Be-Ch
95-16	Sundance	E. Sheep Mtn	S, K, Be-Ch, G
95-15	Sundance	E. Sheep Mtn	Be-Ch, G, S
95-14	Sundance	Cody	G, K, Be-Ch, S
93-1	Sundance	N. Sheep Mtn	K, S, Be-Ch, G
95-11	Sundance	Cody	G, K, Be-Ch, S
95-57	Sundance	Lander Dome	Sm, G, K
95-56	Sundance	Lander Dome	Sm, K, Be-Ch

Notes: G = glauconite, I = illite, K = kaolinite, Ch = discrete chlorite, Co = corrensite, B-C = berthierine/chamosite (7–14 Å chlorite), S = smectite. Approximate stratigraphic position is represented, with lowermost Upper Sundance sandstones at the base of the table and uppermost Upper Sundance sandstones to the top, below overlying basal Morrison sandstones.

TABLE 2. SEM-EDS analyses of chlorites presented as elemental ratios

Sample no.	Morphology	Fe/(Fe+Mg)	Al:Fe	Al:Mg
95-56	honeycomb	0.69	2.66	5.79
95-56	honeycomb	0.67	8.52	17.61
95-56	honeycomb	0.76	1.21	3.81
95-56	honeycomb	0.68	2.06	4.40
	MEAN	0.70	3.62	7.90
	STD DEV	0.04	3.33	6.53
95-39	5 mm platelet	0.98	0.11	5.87
95-39	5 mm platelet	0.90	0.40	3.49
95-39	5 mm platelet	0.97	0.20	5.74
	MEAN	0.95	0.24	5.03
	STD DEV	0.04	0.14	1.34
93-1	rosettes	0.87	0.69	4.45
95-16	rosettes	0.90	0.85	7.76
95-16	rosettes	0.82	1.38	6.20
95-16	rosettes	0.81	1.39	5.98
95-16	rosettes	0.84	1.18	6.40
95-39	rosettes	0.79	0.84	3.22
95-41	rosettes	0.70	1.86	4.31
95-41	rosettes	0.76	1.11	3.56
95-41	rosettes	0.71	1.72	4.16
	MEAN	0.80	1.22	5.12
	STD DEV	0.07	0.40	1.53

Note: Results for each specimen represent the average of 10 spot analyses.

dered *IIb* (Fig. 5B), which is identified by broad peaks at 2.59–2.55 and 2.45–2.39 Å (e.g., Moore and Reynolds 1997; Roberson, et al. 1999). It is similar to disordered *IIb* corrensite in lacustrine and evaporite-associated mudrocks from the Devonian Orcadian Basin (Hillier 1993) and in Miocene-Pleistocene sediments associated with evaporites from the Dead Sea Rift (Sandler et al. 2001). Fe/(Fe + Mg) ratios of Sundance corrensite are 0.70–0.75 (Table 2), Al:Fe ratios are 1.21–8.52 (mean = 3.62), and crystals occur as crenulated boxwork or honeycomb pore linings that are isopachous (Fig. 5C). This texture is similar to those of swelling chlorites, saponites, and corrensites studied by Humphreys et al. (1989, 1994) and Hillier (1994).

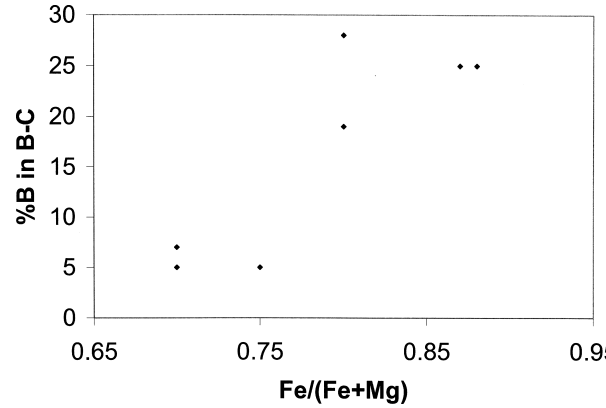

FIGURE 4. Relationship between Fe and Mg concentrations in B-C, expressed as Fe/(Fe + Mg), and percentage of 7 Å B layers expressed as B/(B + C).

Clay minerals in the overlying Morrison formation

Basal Morrison Formation sandstones in the study area are dominated by dioctahedral smectite (Fig. 2) with lesser amounts of kaolinite and illite.

Glauconite

XRD analyses indicate that glaucony grains are dominated by 10 Å glauconite with <10% expandable layers (Fig. 6A). The polytype is disordered *trans*-vacant 1*M* as indicated by weak peaks at 3.74 and 3.06 Å (Moore and Reynolds 1997) (Fig. 6A). Some glaucony specimens also contain a 14 Å mineral that expands to 17 Å with ethylene glycol solvation (Fig. 6A), indicating a smectitic component. Glaucony grains are dark green and 10–200 μm in diameter. SEM-EDS analyses indicate that the finest of the glauconite grains have the lowest K content (3–5 wt% K_2O) and show evidence of dissolution, i.e., they are pitted, non-spherical, and appear to have over growths of wavy smectite on their surfaces. Coarser glauconite grains (e.g., >30 μm) have higher K content (6–8 wt% K_2O) and occur as well-formed and well-preserved spheres that show little or no evidence of dissolution (Fig. 6B).

DISCUSSION

In the Sundance Formation, the occurrence of glauconite as green grains along bedding planes is distinct from that of chlorite minerals as pore-fillings and pore-linings. The glauconite grains most likely were derived by reworking of Sundance sediments in a depositional and geochemical environment that, prior to marine regression, would have resembled glaucony facies of today (Odin 1988; Rao et al. 1993). Marine regression exposed the glaucony facies sediments to increasingly shallower water and stronger currents that led to deposition of reworked glauconite grains along bedding planes in tidal inlets, shoals, and tidal flats (Uhlir et al. 1988).

In contrast, the pore-filling and pore-lining textures of the chlorite minerals indicate that they are authigenic and formed in situ. Conditions in the Sundance tidal inlets, shoals, and tidal flats would have been very similar to those in modern sedimentary environments that foster formation of the verdine fa-

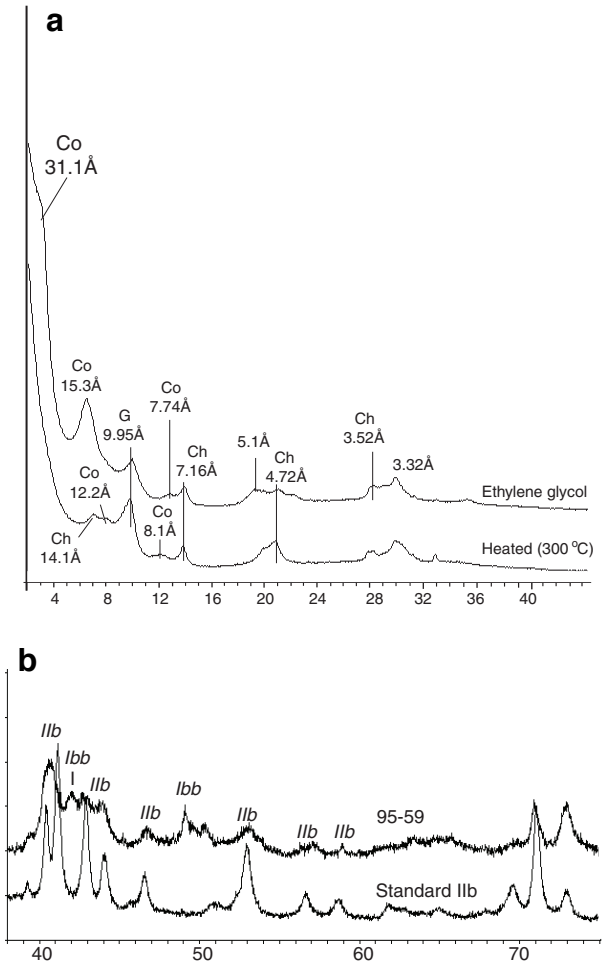

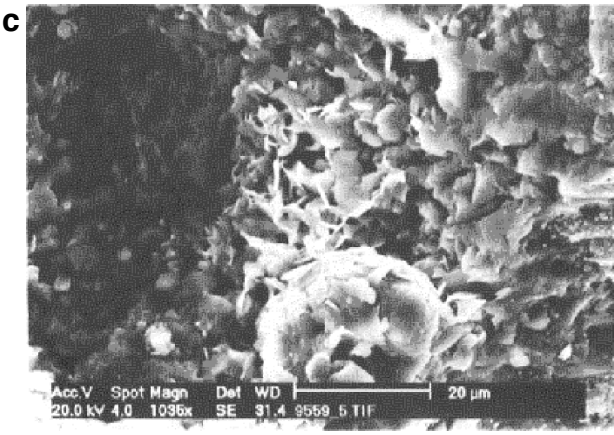

FIGURE 5. (**a**) XRD data from oriented mounts of the <1 µm fraction from sample 95-51, a corrensite-bearing sandstone from the uppermost upper Sundance Formation. The top pattern shows expansion to 31.1 Å in the presence of ethylene glycol vapor, with corrensite 002 and 004 peaks at 15.3 and 7.74 Å, respectively. The bottom pattern is the same oriented powder heated to 300 °C for 1 hour. Peaks at 12.2 and 8.1 Å are 002 and 003 peaks produced by collapse to a 24 Å dehydrated corrensite (Roberson et al. 1999). Characteristic peaks are indicated by Co (corrensite), Ch (discrete chlorite), and G (glauconite). Co$K\alpha$ radiation. (**b**) Disordered *IIb* polytype associated with Sundance Formation corrensite. A metamorphic *IIb* chlorite with well-defined peaks (CYCR, from the Macaulay Institute collection) is presented for comparison. Note the presence of *Ibb* chlorite polytype peaks 2.50 and 2.13 Å. The pattern shown for 95-59 was produced by digitally subtracting a glauconite pattern from a XRD pattern of the <1 µm fraction of 95-59. Data obtained from spray-dried powders. Co$K\alpha$ radiation. (**c**) SEM image of pore-lining, flaky-to-honeycomb-like corrensite and discrete chlorite, sample 95-59.

cies: slightly reducing, pH = 7.5–8.5, T = 25 °C, brackish to normal marine salinity, sandy substrate, and high sedimentation rate. The micro-reducing environments required for formation of odinite, such as cavities in bioclasts (Bailey 1988a; Odin 1988, 1990), were present in Sundance sands (Brenner et al. 1985; Uhlir et al. 1988). Accordingly, we propose that the B-C of the Sundance Formation results from early diagenetic transformation of precursor odinite of the verdine facies. The interpretation that odinite initially formed at the sediment-seawater interface and subsequently dissolved and recrystallized into interstratified B-C is similar to interpretations given by Ehrenberg (1993), Hillier (1994), Hornibrook and Longstaffe (1996), and Ryan and Reynolds (1996). This interpretation is also supported by observations of Bailey (1988a), who found that odinite is unstable in geochemical conditions that differ from its restricted environment of formation. At shallow burial depths of only 10 m, odinite transforms to a more chlorite-like 7–14 Å mineral of the Iba polytype (Bailey 1988a). The transformation of poorly crystalline, Fe-rich 7 Å precursors to chlorite in laboratory experiments, and the appearance of grain-coating chlorite derived from similar precursors at 90 °C in North Sea sandstones (Aagaard et al. 2000), also supports this interpretation. The very Fe-rich platelets of clay observed in sample 93-39 may be analogous to the poorly crystalline B-C precursors documented by Aagaard et al. (2002). However, our data do not contain information on the mineralogical and structural nature of these clays and thus precludes further analysis of this issue.

The presence of authigenic corrensite and discrete chlorite in the uppermost Upper Sundance indicates geochemical conditions at this stratigraphic level that differed from those in B-C-bearing lower parts of the Sundance Formation. We propose that the differences were created by regression of the Sundance Sea. Reducing conditions required for the formation of Fe^{+2}-bearing B-C (from precursor odinite) must have persisted in all but the uppermost Upper Sundance, otherwise B-C (or precursor odinite) likely would have decomposed in the presence of oxidizing groundwater. Aeolian and evaporitic coastal plain deposits of the basal part of the overlying Morrison Formation (Imlay 1980; Uhlir et al. 1988) imply the presence of oxidizing, perhaps evaporitic brines that presumably infiltrated the uppermost Sundance sands during marine regression. These oxidizing groundwaters would have caused dissolution of odinite in the upper few meters of Sundance sands given its instability in geochemical conditions that differ from its restricted environment of formation (Bailey 1988a; Odin 1990).

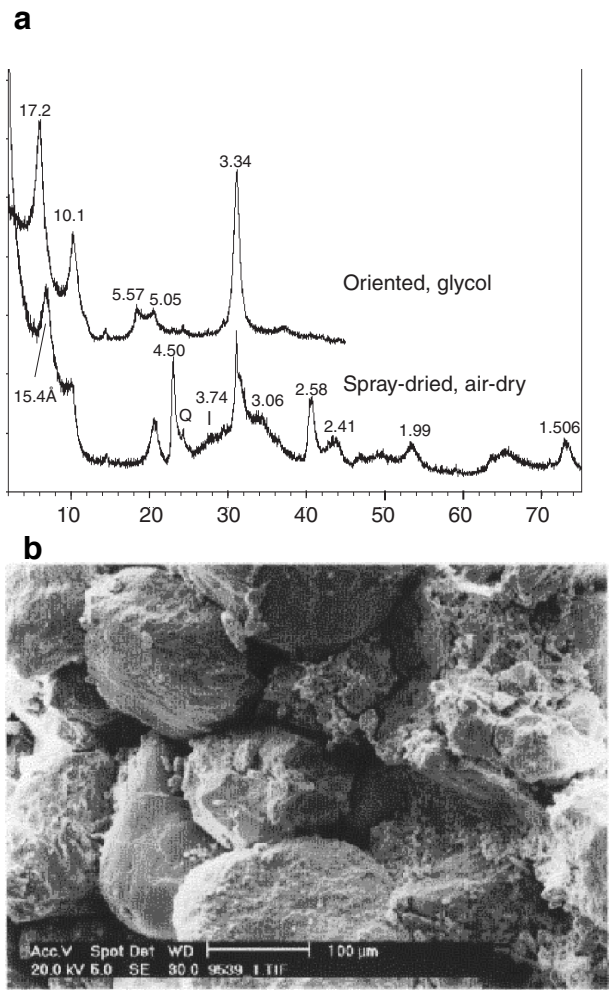

FIGURE 6. (**a**) XRD analyses of glauconite from the <1 µm fraction of 95-39, the most glauconite-rich sample analyzed in this study. The top pattern is of the oriented and ethylene glycol-solvated <1 µm fraction, the bottom pattern is of the spray-dried, air-dried <1 µm powder. These patterns are typical of Sundance glauconite, and indicate predominance of a 10 Å, disordered *tv-1M* structure. The 17 Å peak is smectite and it occurs on the surface of glauconite grains and in pore space. Quartz is indicated in both patterns by the peaks at 4.26 Å and 3.34 Å (composite quartz-glauconite peak). Co*K*α radiation. (**b**) SEM image of glauconite clasts along a bedding lamination, sample 95-39.

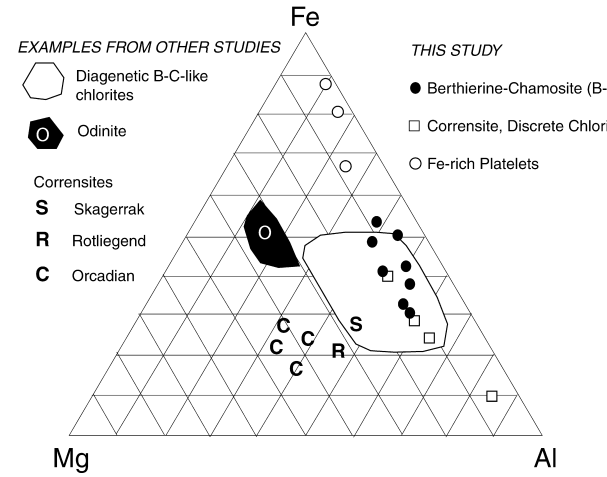

FIGURE 7. Ternary diagram after Velde (1985) and Humphreys et al. (1989). Note similarity between Sundance B-C and other similar sedimentary berthierine-chamosite (B-C)-like chlorites, as well as the difference between Sundance corrensite and those reported in the literature (Skagerrak, Rotliegend, and Orcadian). B-C compositions are from Jahren and Aagaard (1989), Hillier (1994), Hornibrook and Longstaffe (1996), and Ryan and Reynolds (1996). Odinite data are from Bailey (1988a). For saponites and corrensites, Skagerrak data are from Humphreys et al. (1989), Orcadian data are from Hillier (1993), and Rotliegend data are from Hillier (1994).

Under this scenario, odinite dissolution was followed by crystallization of saponite, a precursor to diagenetic corrensite in some sabkha, aeolian, and evaporite-associated sedimentary rocks (Bodine and Madsen 1987; Hillier 1993; Sandler et al. 2001). This interpretation is supported by the presence of saponite and corrensite in evaporite-associated sandstones of the Permian Rotliegend and Yates Formations and the Jurassic Norphlett Formation (Dixon et al. 1989; Janks et al. 1992; Platt 1993; Hillier 1994) that show distinctive similarities to Sundance corrensite with regard to both texture (boxwork/honeycomb pore-linings) and mineralogy (corrensite and the *IIb* polytype). Similar oxidation and reduction processes have been attributed to the formation of rosettes of chamosite and honeycomb-like pore-linings of Mg-rich swelling chlorite in sandstones of the Late Triassic Skagerrak Formation (central North Sea). Chamosite rosettes occur in shallow- to marginal-marine sandstones whereas swelling chlorite, perhaps a mixture of saponite and corrensite, was found in associated fluvial sandstones (Humphreys et al. 1989). In the case of the Sundance Formation, burial diagenesis at temperatures of 90–120 °C caused transformation of saponite to corrensite and discrete chlorite, a reaction series that has been documented in evaporite-associated sequences elsewhere (April 1981; Hillier 1993, 1994; Sandler et al. 2001).

Compositionally, Sundance B-C is very similar to B-C and chamositic pore-lining chlorites from numerous other sandstones (Fig. 7). However, Sundance corrensite differs somewhat from other examples of corrensites in sandstones associated with evaporites (e.g., Rotliegend, Norphlett, Yates, Skagerrak Formations), particularly with respect to values of Fe/(Fe + Mg). In particular, the Fe/(Fe + Mg) range of 0.70–0.75 for Sundance corrensite and discrete chlorite is high when compared to "swelling chlorites" and corrensites from these other formations, which typically range from 0.3 to 0.7 (Curtis et al. 1985; Bettison and Schiffman 1988; Hluchy 1988; Dixon et al. 1989; Humphreys et al. 1989; Janks et al. 1992; Hillier 1993, 1994). We attribute the relatively high Fe content of Sundance corrensite (Fig. 7) to the predicted Fe-rich nature of the odinite that likely preceded crystallization of saponite. Yet, although Fe/(Fe + Mg) values of Sundance corrensite are greater than most sedimentary corrensites, they are slightly less than Fe/(Fe + Mg) of most Sundance B-C specimens, which range from 0.70–0.87. If marine regression-related groundwaters were

produced in sabkha or evaporitic environments, they probably would have been elevated in Mg (Bodine and Madsen 1987), and could have produced saponite with lower Fe/(Fe + Mg) than precursor odinite, but higher Fe/(Fe + Mg) than most sedimentary corrensites.

A plot of Fe/(Fe + Mg) vs. %B layers produces a linear correlation coefficient of 0.64 (Fig. 4), indicating a moderate correlation between Fe-Mg content and %B layers. Previous studies (e.g., Hillier 1994; Ryan and Reynolds 1996) have indicated that %B is controlled by temperature, and that with increasing temperature, B layers transform to C layers. However, those studies were carried out on B-C specimens from sandstones exposed to a wider temperature range of approximately 90–200 °C (compared to ≤120 °C for Sundance sandstones). At the lower end of this temperature range (90–140 °C), %B layers do not vary systematically with temperature and range from 11–26%. However, at temperatures between 140 and 200 °C, %B progressively decreases from 10 to 0% with increasing depth and temperature. The wide ranges in B-C interstratification and composition in the Sundance are not surprising considering that metastable assemblages are quite common in sedimentary rocks exposed to low-middle grade diagenetic conditions (Yeh and Savin 1977; Sheppard and Gilg 1996). The presence of *Ibb* and disordered *IIb*, and the lack of *Iaa* and ordered *IIb* polytypes, is consistent with a burial depth of <4000 m and maximum diagenetic temperatures of 90–120 °C. Transformations of *Ibb* → *Iaa*, *Ibb* → *IIb*, and disordered *IIb* → ordered *IIb* in sedimentary rocks are believed to require temperatures of 120–200 °C (Hillier 1994; Spotl et al. 1994; Ryan and Reynolds 1996).

Summary remarks

Glauconite, B-C, and corrensite are all documented here to occur in the Sundance Formation, the first such documentation in a single formation. Recognition of this assemblage is important because these Fe-rich clays each form under different depositional and early diagenetic conditions. The presence of allochthonous glauconite reflects reworking of mature glauconite grains that initially formed in deep water (>100 m) and were subsequently eroded from the seafloor, transported landward, and deposited in a shallow-marine environment. The geochemical conditions of this shallow-marine environment must have been similar to the Holocene verdine facies, an environment that fosters formation of disordered, Fe-rich 7 Å clay (odinite) at the sediment-seawater interface. Subsequent burial in the marine environment appears to cause transformation of odinite to B-C. However, where pore water conditions change to oxidizing and possibly evaporitic during marine regression, it appears that oxidized groundwater can penetrate former marine sands and cause oxidation of odinite clays of the verdine facies to saponite. During subsequent burial diagenesis, saponite undergoes transformation to corrensite and, ultimately, discrete chlorite. The presence of *Ibb* B-C and disordered *IIb* corrensite are consistent with diagenetic conditions that did not exceed 4000 m burial and 120 °C.

Recognition of glauconite, B-C, and corrensite in sandstones has significant potential for facies interpretations, particularly where fossil or sedimentologic data are either lacking or insufficient to allow paleoenvironmental interpretation, as might be the case with Precambrian sandstones. Future studies of similar sandstones with well-constrained sequence stratigraphic records may help to further constrain the conditions that favor formation of Fe-rich clays.

Acknowledgments

We thank E. Paterson, M. Roe, D. Duthie, and C. Thomsen of the Macaulay Institute, H. Carlson of Middlebury College, J. Swierc of the Helena College of Technology, and Gary Johnson of Dartmouth College for assisting with various aspects of this project. Thorough reviews by J. Aronson, H. Roberson, and an anonymous reader are greatly appreciated. Funding was provided by the National Science Foundation (NSF-AMP and CCLI), Middlebury College, and the Macaulay Land Use Research Institute.

References cited

Aagaard, P., Jahren, J.S., Harstad, A.O., Nilsen, O., and Ramm, M. (2000) Formation of grain-coating chlorite in sandstones; laboratory synthesized vs. natural occurrences. Clay Minerals, 35, 261–269.

Ahn, J.H. and Peacor, D.R. (1985) Transmission electron microscopic study of diagenetic chlorite in Gulf Coast argillaceous sediments. Clays and Clay Minerals, 33, 228–237.

Amouric, M., Parron C., Casalini, L., and Giresse, P. (1995) A (1:1) 7-Å Fe phase and its transformation in Recent sediments: an HRTEM and AEM study. Clays and Clay Minerals, 43, 446–454.

April, R.H. (1981) Trioctahedral smectite and interstratified chlorite/smectite in Jurassic strata of the Connecticut Valley. Clays and Clay Minerals, 29, 31–39.

Bailey, S.W. (1988a) Odinite, a new dioctahedral-trioctahedral Fe^{3+}-rich 1:1 clay mineral. Clay Minerals, 23, 237–247.

———(1988b) Chlorites: structures and crystal chemistry. In S.W. Bailey, Ed., Hydrous Phyllosilicates (Exclusive of Micas), 19, 347–403. Reviews in Mineralogy, Mineralogical Society of America, Washington, D.C.

Banfield, J. F. and Bailey, S.W. (1996) Formation of regularly interstratified serpentine-chlorite minerals by tetrahedral inversion in long-period serpentine polytypes. American Mineralogist, 81, 79–91.

Bettison, L.I. and Schiffman, P. (1988) Compositional and structural variations of phyllosilicates from the Point Sal ophiolite, California. American Mineralogist 73, 62–76.

Bodine, M.W. Jr. and Madsen, B.M. (1987) Mixed-layer chlorite/smectites from a Pennsylvanian evaporite cycle, Grand County, Utah. Proceedings, International Clay Conference, 8, 85–93.

Brenner, R.L, Swift, D.J.P., and Gaynor, G.C. (1985) Re-evaluation of coquinoid sandstone depositional model, Upper Jurassic of central Wyoming and south-central Montana. Sedimentology, 32, 363–372.

Cathelineau, M. and Nieva, D. (1985) A chlorite solid solution geothermometer; the Los Azufres (Mexico) geothermal system. Contributions to Mineralogy and Petrology, 91, 235–244.

Chen, Z.Q. (1989) A fission track study of the terrigenous sedimentary sequences of the Morrison and Cloverly Formations in the Northeastern Bighorn Basin, Wyoming. Ph.D. Dissertation, Dartmouth College, Hanover, N.H.

Curtis, C.D., Hughes, C.R., Whiteman, J.A., and Whittle, C.K. (1985) Compositional variation within some sedimentary chlorites and some comments on their origin. Mineralogical Magazine, 49, 375–386.

de Caritat, P., Hutcheon, I., and Walshe, J.L. (1993) Chlorite geothermometry: A review. Clays and Clay Minerals, 41, 219–239.

Dixon, S.A., Summers, D.M., and Surdam, R.C. (1989) Diagenesis and preservation of porosity in Norphlet Formation (Upper Jurassic), southern Alabama. The American Association of Petroleum Geologists Bulletin, 73, 707–728.

Drever, J.I. (1973) The preparation of oriented clay mineral specimens for X-ray diffraction analysis by a filter-membrane peel technique. American Mineralogist, 50, 741–751.

Ehrenberg, S.N. (1993) Preservation of anomolously high porosity in deeply buried sandstones by grain-coating chlorite: examples from the Norwegian Continental Shelf. The American Association of Petroleum Geologists Bulletin, 77, 1260–1286.

Hillier, S. (1993) Origin, diagenesis, and mineralogy of chlorite minerals in Devonian lacustrine mudrocks, Orcadian Basin, Scotland. Clays and Clay Minerals, 41, 240–259.

———(1994) Pore-lining chlorites in siliciclastic reservoir sandstones: electron microprobe, SEM, and XRD data, and implications for their origin. Clay Minerals, 29, 665–679.

———(1999) Use of an air brush to spray dry samples for X-ray powder diffraction, Clay Minerals, 34, 127–135.

Hluchy, M.M. (1988) The chemistry of clay minerals associated with evaporites in New York and Utah. Ph.D. Dissertation, Dartmouth College, Hanover, NH.

Hornibrook, E.R.C. and Longstaffe, F.J. (1996) Berthierine from the Lower Creta-

ceous Clearwater Formation, Alberta, Canada. Clays and Clay Minerals, 44, 1–21.
Humphreys, B., Smith, S.A., and Strong, G.E. (1989) Authigenic chlorite in Late Triassic sandstones from the Central Graben, North Sea. Clay Minerals, 24, 427–444.
Humphreys, B., Kemp, S.J., Lott, G.K., Bermanto, Dharmayanti, D.A., and Samsori, I. (1994) Origin of grain-coating chlorite by smectite transformation: an example from Miocene sandstones, North Sumatra back-arc basin, Indonesia. Clay Minerals, 29, 681–692.
Imlay, R.W. (1980) Jurassic paleobiogeography of the conterminous United States in its continental setting. U. S. Geological Survey Professional Paper, P 1062.
Jahren, J.S. and Aagaard, P. (1989) Compositional variations in diagenetic chlorites and illites, and relationships with formation-water chemistry. Clay Minerals, 24, 157–170.
Janks, J. S., Yusas, M.R., and Hall, C.M. (1992) Clay mineralogy of an interbedded sandstone, dolomite, and anhydrite; the Permian Yates Formation, Winkler County, Texas. In D.W. Houseknecht, E.D. Pittman, Eds., Origin, diagenesis, and petrophysics of clay minerals in sandstones, Special Publication, Society of Economic Paleontologists and Mineralogists, 47, 145–157.
Jiang, W.-T., Peacor, D.R., and Buseck, P.R. (1994) Chlorite geothermometry?—contamination and apparent octahedral vacancies. Clays and Clay Minerals, 42, 593–605.
Karpova, G.V. (1969) Clay mineral post-sedimentary ranks in terrigenous rocks. Sedimentology, 13, 5–20.
Kronen, J.D., Jr. and Glenn, C.R (2000) Pristine to reworked verdine; keys to sequence stratigraphy in mixed carbonate-siliciclastic forereef sediments (Great Barrier Reef). In C.R. Glenn, L. Prevot-Lucas, and J. Lucas, Eds., Marine authigenesis; from global to microbial, Special Publication, Society for Sedimentary Geology, 66, 387–403.
McCarty, D.K. and Reynolds, R.C. Jr. (1995) Rotationally disordered illite/smectite in Paleozoic K-bentonites. Clays and Clay Minerals, 43, 271–284.
Moore, D.M. and Reynolds, R.C. Jr. (1997) X-ray diffraction and the identification and analysis of clay minerals, Second Ed. Oxford University Press, New York.
Odin, G.S. (1985) La "verdine", facies granulaire vert, marin et cotier distinct de la glauconie: distribution actuelle et composition. Compte Rendus, Academie des Sciences Paris, 301, II(2), 105–118.
———(1988) Green Marine Clays, Developments in Sedimentology 45. Elsevier, Amsterdam.
———(1990) Clay mineral formation at the continent-ocean boundary: the verdine facies. Clay Minerals, 25, 477–483.
Odin, G.S. and Giresse, P. (1972) Formation de mineraux phylliteux (berthierine, smectites ferriferes, glauconite ouverte) dans les sediments du Golfe de Guinee; Formation of phyllitic minerals (berthierine, ferriferous smectites, glauconite) in the sediments of the Gulf of Guinea. Comptes Rendus Hebdomadaires des Seances de l'Academie des Sciences, Serie D: Sciences Naturelles, 275, 177–180.
Odin, G.S. and Sen Gupta, B.K. (1988) Geological significance of the verdine facies. In G.S. Odin, Ed., Green Marine Clays, Developments in Sedimentology, 45, p. 205–219. Elsevier, Amsterdam.
Odin G.S., Bailey S.W., Amouric M., Frohlich F., and Waychunas G.A. (1988) Mineralogy of the facies verdine. In G.S. Odin, Ed., Green Marine Clays, Developments in Sedimentology, 45, p. 159–204. Elsevier, Amsterdam.
Peterson, J.A. (1957) Marine Jurassic of northern Rocky Mountains and Williston Basin. The American Association of Petroleum Geologists Bulletin, 41, 339–440.
Picard, M.D. (1993) The early Mesozoic history of Wyoming. Geological Survey of Wyoming, Memoir 5, 211–248.
Platt, J.D. (1993) Controls on clay mineral distribution and chemistry in the Early Permian Rotliegend of Germany. Clay Minerals, 28, 393–416.
Porrenga, D.H. (1967) Glauconite and chamosite as depth indicators in the marine Environment. Marine Geology 5, 495–501.
Rao, P.V., Thamban, M., Lamboy, M. (1995) Verdine and glaucony facies from surficial sediments of the eastern continental margin of India. Marine Geology, 127, 105–113.
Reynolds, R.C. Jr. (1985) NEWMOD© A computer program for the calculation of one-dimensional diffraction profiles of clays. Published by the author, 8 Brook Road, Hanover, New Hampshire.
———(1988) Mixed layer chlorite minerals. In S.W. Bailey, Ed., Hydrous Phyllosilicates (Exclusive of Micas), 19, 601–629. Reviews in Mineralogy, Mineralogical Society of America, Washington, D.C.
———(1993) WILDFIRE© A computer program for the calculation of three-dimensional diffraction profiles of clays. Published by the author, 8 Brook Road, Hanover, New Hampshire.
Reynolds, R.C. Jr., DiStefano, M.P., and Lahann, R.W. (1992) Randomly interstratified serpentine/chlorite: its detection and quantification by powder X-ray diffraction methods. Clays and Clay Minerals, 40, 262–267.
Roberson, H.E., Reynolds, R.C. Jr., and Jenkins, D.M. (1999) Hydrothermal synthesis of corrensite; a study of the transformation of saponite to corrensite. Clays and Clay Minerals, 47, 212–218.
Ryan, P.C. and Reynolds, R.C. Jr. (1996) The origin and diagenesis of grain-coating serpentine-chlorite in Tuscaloosa Formation sandstone, U.S. Gulf Coast. American Mineralogist, 81, 213–225.
Sandler, A., Nathan, Y., Eshet, Y., and Raab, M. (2001) Diagenesis of trioctahedral clays in a Miocene to Pleistocene sedimentary-magmatic sequence in the Dead Sea Rift, Israel. Clay Minerals, 36, 29–48.
Shata, S. and Hesse, R. (1998) A refined XRD method for the determination of chlorite composition and application to the McGerrigle Mountains anchizone in the Quebec Appalachians. Canadian Mineralogist, 36, 1525–1546.
Sheppard, S.M.F. and Gilg, H.A. (1996) Stable isotope geochemistry of clay minerals. Clay Minerals, 31, 1–24.
Spotl, C., Houseknecht, D.W., and Longstaffe, F.J. (1994) Authigenic chlorites in sandstones as indicators of high-temperature diagenesis, Arkoma Foreland Basin, USA. Journal of Sedimentary Research, A64, 553–566.
Steidtmann, J.R. (1993) The Cretaceous foreland basin and its sedimentary record. Geological Survey of Wyoming Memoir 5, 250–271.
Swierc, J.E. and Johnson, G.D. (1996) A local chronostratigraphy for the Morrison Formation, Northeastern Bighorn Basin, Wyoming. Wyoming Geological Association Guidebook, 47, 315–327. Wyoming Geological Association, Laramie.
Uhlir, D.M. (1987) Sedimentology of the Sundance Formation, northern Wyoming. Ph.D. Dissertation, Iowa State University, Ames.
Uhlir, D.M., Akers, A., and Vondra, C.F. (1988) Tidal inlet sequence, Sundance Formation (Upper Jurassic), north-central Wyoming. Sedimentology, 35, 739–752.
Velde, B. (1985) Clay Minerals: A Physico-Chemical Explanation of their Occurrence. Developments in Sedimentology, 40. Elsevier, Amsterdam.
Wiewiora, A., Giresse, P., Jaunet, A.M., Wilamowski, A., and Elsass, F. (1999) Crystal chemistry of layer silicates of the Miocene Green Grain (Congo Basin) from transmission electron microscopy (TEM) and analytical electron microscopy (AEM) observation. Clays and Clay Minerals, 47, 582–590.
Yeh, H.-W. and Savin, S.M. (1977) The mechanism of burial metamorphism of argillaceous sediments: Oxygen isotope evidence. Geological Society of America Bulletin, 88, 1321–1330.

MANUSCRIPT RECEIVED JUNE 30, 2001
MANUSCRIPT ACCEPTED JULY 9, 2002
MANUSCRIPT HANDLED BY JAMES ARONSON